Proceedings of the ASME 2022 International Design Engineering Technical Conferences & Computers and Information in Engineering Conference
IDETC/CIE 2022
August 14-August 17, 2022, St. Louis, United States

DETC2022-XXXX

COMPACT TIME DOMAIN NMR DESIGN FOR THE DETERMINATION OF HYDROGEN CONTENT IN GAS TURBINE FUELS

Jacob Martin *
Department of Mech. Eng.
Department of Physics and Astronomy
University of South Carolina
Columbia, South Carolina 29201
Email: jsmartin@email.sc.edu

Austin Downey
Department of Mech. Eng.
Department of Civil, Const. and Env.
University of South Carolina
Columbia, South Carolina 29201

Sang Hee Won
Department of Mech. Eng.
University of South Carolina
Columbia, South Carolina 29201

ABSTRACT

Low-resolution nuclear magnetic resonance is a tool that has been employed for many years as an effective method for analyzing complex materials in a non-destructive fashion. This work has been aimed at the development of a prototype compact NMR system with the potential to be utilized for simple and rapid in situ measurements of key properties of jet fuels. The compact system consists of a neodymium magnet configuration with a field strength of 0.645 T, custom printed circuit boards, and radio frequency electronics. It is driven by a National Instruments PXI chassis fitted with modules that control the excitation and detection of hydrogen proton resonance in various samples. The current system is suitable for transverse relaxation (T2) studies using the Carr-Purcell-Meiboom-Gill pulse sequence, as it can produce relaxation curves containing thousands of spin echoes. Determination of hydrogen content (mass %), which is strongly correlated to combustion properties of fuels, is the primary area of interest for this study. Utilizing an array of 16 reference samples, a direct correlation between initial signal amplitude and hydrogen density (kmol/m^3) was established. This relationship, along with mass density measurements, was used to determine hydrogen content in six different jet fuels. The maximum error between measured and accepted values for the fuels was 0.7%.

*Address all correspondence to this author.

INTRODUCTION

The determination of physical and chemical properties of petroleum distillates is important when it comes to controlling fuel quality and performance. The standard methods by which fuel properties are acquired are documented by the American Society for Testing and Materials (ASTM) in the United States. ASTM methods are commonly accepted and used, but depending on the parameter being tested for, procedures have often involved long sample preparation time and may alter or destroy the test sample entirely. As a result of this, alternative methods that offer fast and noninvasive tests with essentially no sample preparation is highly sought after.

Nuclear magnetic resonance (NMR) has emerged as one of the most common and powerful alternative methods for fuel property (not to be confused with "alternative fuels") analysis, comprised of three main areas: time-domain NMR (TD-NMR), NMR spectroscopy, and magnetic resonance imaging (MRI). Devices that utilize cryogenic cooling to create strong magnetic fields (high-field devices) can provide the most high resolution data, but they are limited in many applications due to their size and operating requirements. However, the implementation of permanent magnets in NMR (low-field devices) can overcome these limitations through the ability to create compact and robust systems with short measurement times [1]. TD-NMR is especially attractive, as it is the simplest method and can afford a large variability in design. These devices can measure the T2 re-

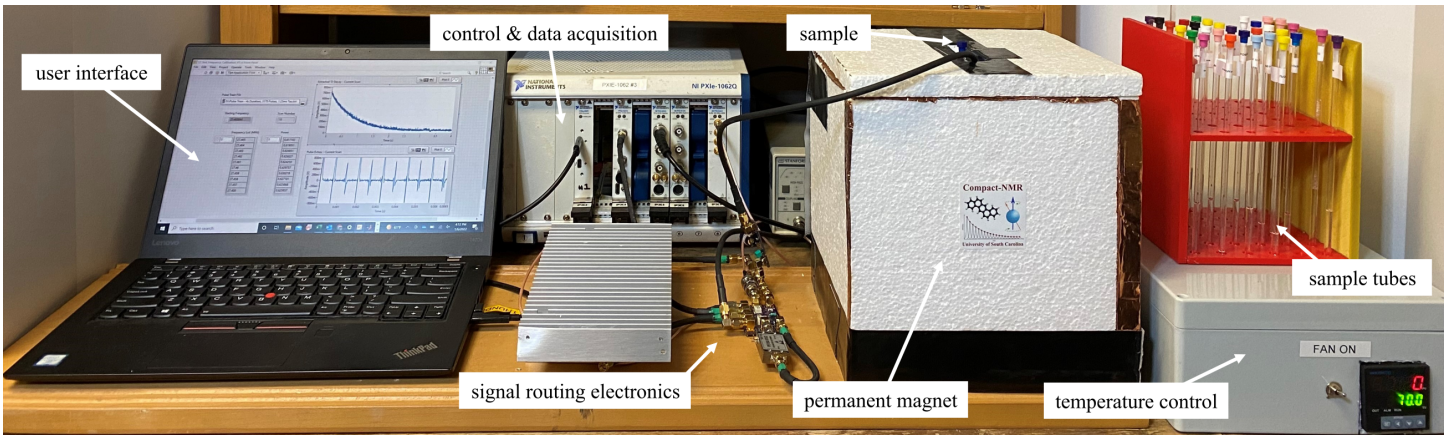

FIGURE 1. FULL EXPERIMENTAL SETUP FOR THE DESKTOP TD-NMR SYSTEM.

laxation curves of liquid samples using a Carr-Purcell-Meiboom-Gill pulse sequence [2], where the data is most often processed using inverse Laplace transform (ILT) and regression methods to extract decay rates. Work done by Barbosa et. al has shown the ability of commercial TD-NMR devices to produce correlations between relaxation data and relative hydrogen index with viscosity, API gravity, refractive index, molecular weight, and correlation index [3–5]. Other applications of TD-NMR in fuel analysis have included the estimation of aromatic content in petroleum distillates [6], diesel fuel quality monitoring [7], biodiesel content estimation [8], and the examination of intact oilseeds [9].

One of the vital parameters of petroleum distillates is hydrogen content (represented as a mass %). In the case of gas turbine fuels, which are considered middle distillates, hydrogen content is directly related to multiple combustion properties. Since gas turbine fuels are exclusively composed only with hydrocarbons, hyrogen content can be directly converted to hydrogen to carbon molar ratio, which exhibits strong correlation with heat of combustion and aromatic content [10]. Exhaust smoke, soot deposits, and thermal radiation will increase as hydrogen content decreases, which can lead to combustor liner burnout [11]. Therefore, a device capable of performing rapid, in situ fuel property analysis to determine hydrogen content could help prevent engine failure. Methods for determining hydrogen content via high-field ^{1}H NMR spectroscopy have been documented in literature [12,13], but the use of a high-field instrument is not feasible for measurements outside of a lab. ASTM standards D4808 [14], D3701 [15], and D7171 [11] make use of commercial low-field NMR spectrometers, with D7171 being the only relevant one as it uses a pulsed NMR system instead of continuous-wave. Furthermore, the most logical decision for the design of a prototype capable of monitoring hydrogen content in situ would be a pulsed TD-NMR system.

In this work, we present the development of a compact TD-NMR system capable of measuring hydrogen content. The device can perform non-destructive tests that provide easily interpreted results. There is also very little data processing required besides averaging data points between scans of the same material. This study shows the possibility for building simple, robust NMR systems that can be customized for a specific deployment. The contributions of this paper are twofold: (1) demonstrating that a lab-built TD-NMR device can categorize any sample containing hydrogen by its hydrogen density and; (2) demonstrating that a lab-built TD-NMR device can achieve 0.7% error between measured and accepted values for hydrogen content classification of gas turbine fuels.

SYSTEM DESIGN

The desktop system can be seen in Fig 1, and the full schematic is represented in Fig. 3. A laptop running LabVIEW programming software connects to the PXI control chassis via a USB-C cable and is controlled through a custom GUI. The control chassis connects to the signal routing and amplification electronics using 50 Ω coaxial cables with SMA connectors. The permanent magnet is kept in a Styrofoam container with an opening at the top used for exchanging samples and connecting the coil to the signal routing system. Standard 5 mm NMR tubes (Norell XR-55) are used for all sample testing.

Permanent Magnet

The permanent magnet configuration used in this system, shown in Fig. 2(a), is comprised of two dipole cylindrical magnets surrounded by a steel yolk and is similar to the one employed by Sahebjavaher et al. [16]. The grade N42 NdFeB permanent magnet disks (sourced from K & J Magnetics, Inc.) are axially magnetized with a diameter of 76.2 mm (3 in.) and a thickness of 25.4 mm (1 in.). The bare magnets produce a measured flux density of 0.5 T when spaced approximately 15 mm apart. In order to improve homogeneity and increase flux density inside

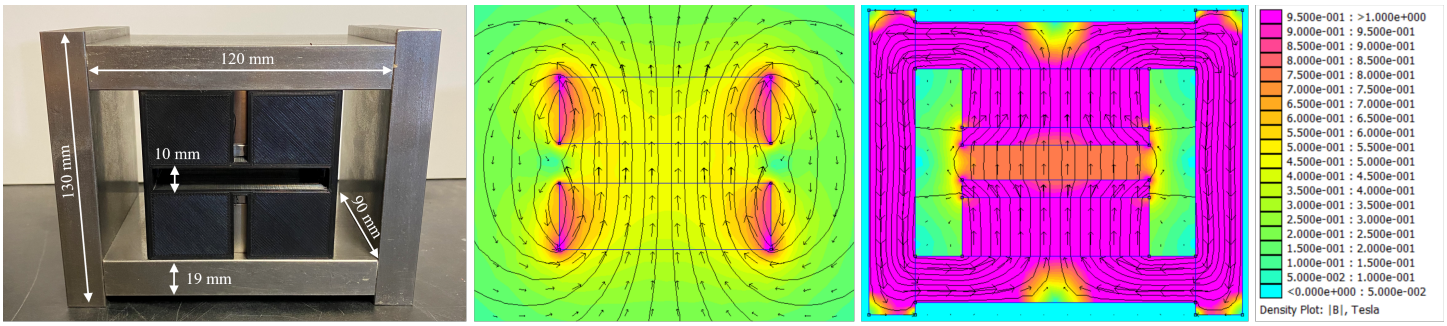

(a) (b) (c)

FIGURE 2. THE CUSTOM PERMANENT MAGNET SHOWING: (A) MAGNET CONFIGURATION; (B) TWO-DIMENSIONAL FINITE ELEMENT SIMULATION USING BARE MAGNETS ONLY, AND; (C) TWO-DIMENSIONAL FINITE ELEMENT SIMULATION OF THE SAME MAGNETS SURROUNDED BY AN IRON YOKE.

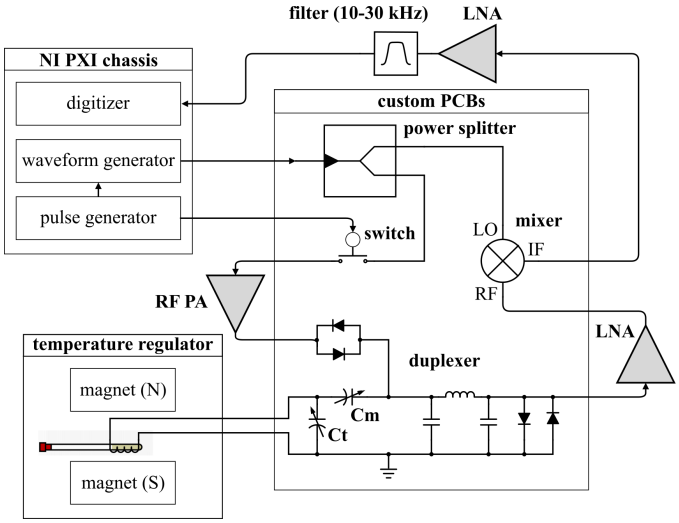

FIGURE 3. FULL SCHEMATIC OF THE CONTROL SYSTEM, PERMANENT MAGNET, AND SIGNAL ROUTING AND AMPLIFICATION ELECTRONICS FOR THE COMPACT TD-NMR SYSTEM.

the gap, the disks are surrounded by 1018 carbon steel bars with a thickness of 19 mm that act as a return path for the magnetic flux. 1018 steel caps with a thickness of 7.5 mm were also placed on the magnet faces for further homogeneity improvements.

Two-dimensional simulations of the magnetic field were performed using the finite element method to verify the improvements before the assembly was completed. For this work, the software package Finite Element Method Magnetics was used to perform the simulations [17]. Fig. 2(b) shows the simulation of the bare magnets and Fig. 2(c) shows the simulation with the steel pieces included. Although FEMM estimated an increase in flux density of roughly 40%, results showed a strength increase of 29% to a maximum value of 0.645 T, which results in a Larmor frequency of about 27.5 MHz. While increasing overall strength and homogeneity, the added steel components also make the design immensely safer, as it confines the majority of the magnetic flux inside its volume. The Styrofoam container that houses the configuration maintains a temperature of 20 °C using a Peltier cooling fan regulated by an industrial temperature controller. The container is also lined with copper tape to help block any outside noise that could interfere with the coil.

Signal Routing and Amplification Electronics

The signal routing and amplification electronics are shown in Fig. 3. Besides the three amplifiers, all of the components are mounted on a custom made PCB. The PCB traces and the ports of each device are all matched to 50 Ω to reduce losses. The power divider starts by splitting a sinusoidal signal, driven at the Larmor frequency, between the mixer and switch. The switch is toggled by a pulse generator to create the pulses needed for sample excitation, which are then amplified up to 35 dBm before the noise blocking diodes. A Pi filter, consisting of a choke and two capacitors, and two Schottky diodes are used to block the high power pulse from the receiving amplifier by acting as a high impedance input during the pulse [18]. The solenoidal coil used to detect the NMR signal is made of 8 turns of 700 µm diameter, Kapton insulated copper wire and fits snugly around the 5mm sample tubes. The coil is matched to 50 Ω at the Larmor frequency using adjustable matching and tuning capacitors, and a Q value of 100 was found by measuring the bandwith of the probe. The sample response signal is amplified by 40 dB using the first low-noise amplifier (LNA) directly after the Schottky diodes. The signal is then shifted into the audio frequency range with a mixer that uses the original sinusoidal wave at the Larmor frequency as the local oscillator. Another stage of 40 dB amplification, along with bandpass filtering from 10-30 kHz, takes place before the signal is sent to a digitizer.

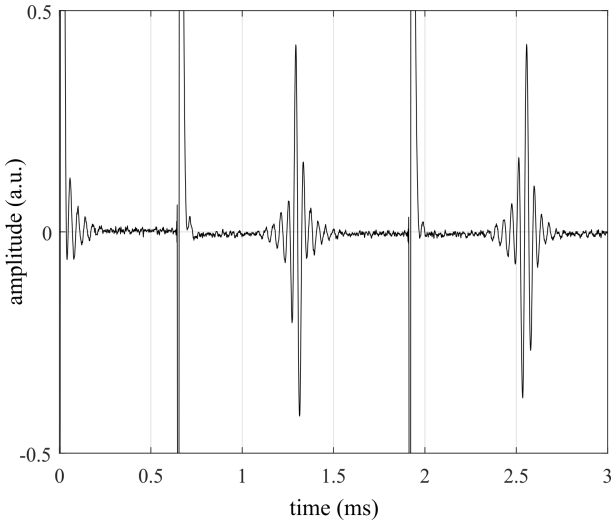

FIGURE 4. TOLUENE SPIN ECHOS RESULTING FROM THE APPLICATION OF ONE 90° PULSE AND TWO 180° PULSES.

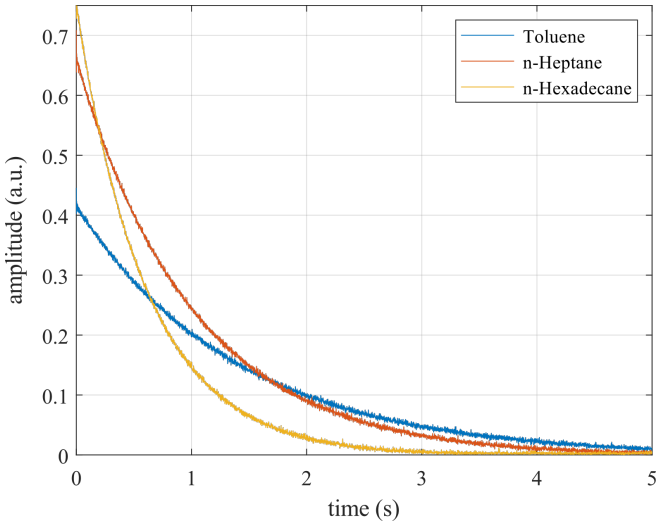

FIGURE 5. T2 RELAXATION CURVES FOR TOLUENE, HEPTANE, AND HEXADECANE FOLLOWING 32 AVERAGES OF 3965 SPIN ECHO PULSES.

Control and Data Acquisition

The control and data acquisition subsystem is made up of an NI PXI chassis fitted with an arbitrary waveform generator, pulse generator, and a 16 to 24-bit digitizer. LabVIEW software was used to create a program capable of controlling excitation and detection, and it employs a GUI in the front end to allow for simple operation of the developed system. The 27.5 MHz carrier signal is synthesized by the arbitrary waveform generator and shaped by the pulse generator, with a 6 μs pulse time corresponding to a 90° flip of the magnetization vector in the sample. The time between the 90° and 180° pulse, commonly referred to as the 'tau' value, is 1.25 ms. Each scan is 5 s in length, with a relaxation delay of 10 s between scans. These values result in a total acquisition time of 4 min for 16 scans. The LabVIEW program is set up to pick out the peak voltage values of the spin echos and plot them as a function of time. This time series can be modeled by the equation:

$$M_{xy}(t) = M_0 \exp(-t/T_2) \tag{1}$$

where $M_{xy}(t)$ is the magnetization at time t, M_0 is the magnetization at equilibrium, and T_2 is the transverse relaxation time.

RESULTS AND DISCUSSION

In order to establish a basis for characterizing arbitrary samples, the system was used to test distilled water and an array of pure liquid hydrocarbons. The pure hydrocarbons included toluene, n-heptane, n-octane, iso-octane, n-dodecane, n-propylbenzene, mesitylene, iso-cetane, n-hexadecane, methylcyclohexane, n-butylcyclohexane, and n-decane. Three mixtures of toluene and heptane were also prepared with mass ratios of 1:3, 1:1, and 3:1 for a total of 16 reference samples. Fig. 4 shows an example of the spin echo signals acquired from a sample of toluene following the application of one 90° pulse and two 180° pulses. The full T_2 relaxation curve can be constructed from the peaks of the spin echos following 3,965 total pulses, as shown for a few samples in Fig. 5.

In order to determine hydrogen content, one can first utilize a general expression for the signal-to-noise ratio of an NMR signal:

$$\mathrm{SNR} \propto N A T^{-1} B_0^{3/2} \gamma_{\mathrm{exc}} \gamma_{\mathrm{obs}}^{3/2} T_2^* n_s^{1/2} \tag{2}$$

where N is the number of molecules, A represents the abundance of active spins, T is temperature, B_0 is the static magnetic field strength, γ_{exc} and γ_{obs} are the gyromagnetic ratios of the excited and observed spins, T_2^* is the effective transverse relaxation time, and n_s is the number of scans for a given sample [19]. Assuming all variables except N and A are held constant, the signal amplitude for different samples should increase directly proportional to the number of hydrogen atoms in the sample (hydrogen density). The theoretical hydrogen density (with units of kmol/m^3) for the reference samples can be calculated using the following:

$$\rho_{\mathrm{H}} = \frac{\rho_{\mathrm{s}} N_{\mathrm{H}}}{M_w} \tag{3}$$

where ρ_{s} is the sample mass density, M_w is the molecular weight, and N_{H} is the number of hydrogen atoms per molecule.

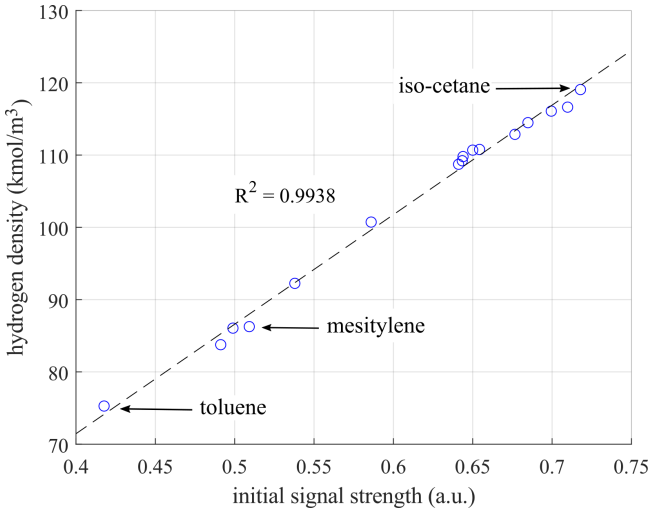

FIGURE 6. LINEAR CORRELATION OF HYDROGEN DENSITY AND INITIAL SIGNAL AMPLITUDE FOR VARIOUS SAMPLES OF PURE HYDROCARBONS.

The hydrogen content can be defined as the ratio of hydrogen density to mass density. Mass density is simple to measure for a given sample. Fig. 6 reports the relationship between hydrogen density and initial signal amplitude for each of the 16 reference samples tested, with select samples annotated. The value used for initial signal amplitude was taken from averaging the first 10 spin echo peaks after 16 total scans of each pure hydrocarbon. Least squares regression was used to create a linear approximation of the data set, which fits well as the R^2 value shows. This linear function can then be used to estimate hydrogen density:

$$\rho_{\mathrm{H}} = 151.5 A_s + 10.84 \tag{4}$$

where A_s is the initial signal amplitude.

Using the linear model presented in Fig. 6, the hydrogen content of an unknown gas turbine fuel can be estimated by solely measuring the initial signal amplitude and mass density. In this work, the hydrogen content was estimated using the signal strength and mass density for six different jet fuels: JP-8 (POSF 10264), Jet-A (POSF 10325), JP-5 (POSF 10289), Shell CPK (POSF 13690), Shell SPK (POSF 5729), and Gevo-ATJ (POSF 10151). The results are shown in Tab. 1 along with the values determined in literature for each [10, 20–22]. Results show that the custom TD-NMR system is quite accurate, as the maximum percent error between measured and accepted hydrogen content values was 0.7%.

TABLE 1. KNOWN AND EXPERIMENTAL HYDROGEN CONTENT VALUES FOR SELECTED JET FUELS.

fuel	known ^{1}H content	measured ^{1}H content	% error
JP-8	14.4	14.5	0.7
Jet-A	14.2	14.1	0.7
JP-5	13.4	13.4	0.0
Shell CPK	14.1	14.0	0.7
Shell SPK	15.5	15.6	0.6
Gevo-ATJ	15.3	15.4	0.6

CONCLUSION

This study shows the potential for building a custom low-field NMR system for the purpose of in situ fuel characterization. A simple, table-top NMR instrument was developed and its capabilities were presented. The permanent magnet setup used to generate a 0.645 T static magnetic field with sufficient homogeneity was shown, along with the signal routing and amplification electronics used to route the excitation and detection signals. The system is quite stable, as it showed a high repeatability for successive testing of identical materials. The instrument demonstrated the direct correlation between hydrogen density and signal amplitude for all reference samples. This relationship was used to make accurate estimations of hydrogen content for six jet fuels, which is an important parameter for determining combustion properties. Tests are quick, non-destructive, and do not require sample preparation or the addition of any reference chemicals. Lab-built systems such as this one can be relatively low-cost and provide valuable insights into the fundamentals of NMR techniques while maintaining a small footprint. In this particular instrument, future work will be dedicated to further scaling down the size and utilizing the T_2 decay curves for structural characterization of fuels.

ACKNOWLEDGMENT

This material was sponsored by the ARO under Grant Number: W911NF-21-1-0306. The views and conclusions contained in this document are those of the authors and should not be interpreted as representing the official policies, either expressed or implied, of ARO or the U.S. Government. The U.S. Government is authorized to reproduce and distribute reprints for Government purposes notwithstanding any copyright notation herein. This work is also partly supported by the University of South Carolina under Grant No. 80004440.

REFERENCES

[1] Nikolskaya, E., and Hiltunen, Y., 2020. "Time-domain nmr in characterization of liquid fuels: A mini-review". *Energy & Fuels,* ***34***(7), pp. 7929–7934.

[2] P. McIntosh, L., 2013. *CPMG*. Springer Berlin Heidelberg, Berlin, Heidelberg, pp. 386–386.

[3] Barbosa, L. L., Kock, F. V. C., Silva, R. C., Freitas, J. C. C., Lacerda, V., and Castro, E. V. R., 2013. "Application of low-field nmr for the determination of physical properties of petroleum fractions". *Energy & Fuels,* ***27***(2), pp. 673–679.

[4] Barbosa, L. L., Kock, F. V., Almeida, V. M., Menezes, S. M., and Castro, E. V., 2015. "Low-field nuclear magnetic resonance for petroleum distillate characterization". *Fuel Processing Technology,* ***138***, pp. 202–209.

[5] Barbosa, L. L., Montes, L. F., Kock, F. V., Morgan, V. G., Souza, A., Song, Y.-Q., and Castro, E. R., 2017. "Relative hydrogen index as a fast method for the simultaneous determination of physicochemical properties of petroleum fractions". *Fuel,* ***210***, pp. 41–48.

[6] Montes, L. F., Oliveira, E. C., lvaro C. Neto, Menezes, S. M., Castro, E. R., and Barbosa, L. L., 2019. "Low-field nmr: A new alternative to determine the aromatic content of petroleum distillates". *Fuel,* ***239***, pp. 413–420.

[7] Santos, P. M., Amais, R. S., Colnago, L. A., Rinnan, ., and Monteiro, M. R., 2015. "Time domain-nmr combined with chemometrics analysis: An alternative tool for monitoring diesel fuel quality". *Energy & Fuels,* ***29***(4), pp. 2299–2303.

[8] da Rocha, G., Colnago, L. A., Moraes, T. B., Zagonel, G. F., de Muniz, G. I. B., Peralta-Zamora, P. G., and Barison, A., 2017. "Determination of biodiesel content in diesel fuel by time-domain nuclear magnetic resonance (td-nmr) spectroscopy". *Energy & Fuels,* ***31***(5), pp. 5120–5125.

[9] Prestes, R. A., Colnago, L. A., Forato, L. A., Vizzotto, L., Novotny, E. H., and Carrilho, E., 2007. "A rapid and automated low resolution nmr method to analyze oil quality in intact oilseeds". *Analytica Chimica Acta,* ***596***(2), pp. 325–329.

[10] Won, S. H., Veloo, P. S., Dooley, S., Santner, J., Haas, F. M., Ju, Y., and Dryer, F. L., 2016. "Predicting the global combustion behaviors of petroleum-derived and alternative jet fuels by simple fuel property measurements". *Fuel,* ***168***, pp. 34–46.

[11] *ASTM D7171-20 (2020) Standard Test Method for Hydrogen Content of Middle Distillate Petroleum Products by Low-Resolution Pulsed Nuclear Magnetic Resonance Spectroscopy*. American Society for Testing Materials: West Conshohocken, PA, 2017.

[12] Mondal, S., Kumar, R., Bansal, V., and Patel, M. B., 2015. "1h nmr method for the estimation of hydrogen content for all petroleum products". *Journal of Analytical Science and Technology,* ***6***(24).

[13] Khadim, M. A., Wolny, R. A., Al-Dhuwaihi, A. S., Al-Hajri, E. A., and Al-Ghamdi, M. A., 2003. "Determination of hydrogen and carbon contents in crude oil and petroleum fractions by nmr spectroscopy". *Arabian Journal for Science and Engineering Section B: Engineering,* ***28***(2A), pp. 147–162. PETROLEUM.

[14] *ASTM D4808-17 (2017) Standard Test Methods for Hydrogen Content of Light Distillates, Middle Distillates, Gas Oils, and Residua by Low-Resolution Nuclear Magnetic Resonance Spectroscopy*. American Society for Testing Materials: West Conshohocken, PA, 2017.

[15] *ASTM D3701-17 (2017) Standard Test Method for Hydrogen Content of Aviation Turbine Fuels by Low Resolution Nuclear Magnetic Resonance Spectrometry*. American Society for Testing Materials: West Conshohocken, PA, 2020.

[16] Sahebjavaher, R. S., Walus, K., and Stoeber, B., 2010. "Permanent magnet desktop magnetic resonance imaging system with microfabricated multiturn gradient coils for microflow imaging in capillary tubes". *Review of Scientific Instruments,* ***81***(2), p. 023706.

[17] Meeker, D., 2010. "Finite element method magnetics". *FEMM,* ***4***(32), p. 162.

[18] Louis-Joseph, A., and Lesot, P., 2019. "Designing and building a low-cost portable ft-nmr spectrometer in 2019: A modern challenge". *Comptes Rendus Chimie,* ***22***(9), pp. 695–711.

[19] Claridge, T. D., 2016. "Chapter 3 - practical aspects of high-resolution nmr". In *High-Resolution NMR Techniques in Organic Chemistry (Third Edition)*, T. D. Claridge, ed., third edition ed. Elsevier, Boston, pp. 61–132.

[20] Nates, S., Carpenter, D., Dryer, F. L., and Won, S. H. *Preferential Vaporization Potential of Jet fuels Evaluated by NMR Spectroscopy*.

[21] Won, S. H., Rock, N., Lim, S. J., Nates, S., Carpenter, D., Emerson, B., Lieuwen, T., Edwards, T., and Dryer, F. L., 2019. "Preferential vaporization impacts on lean blow-out of liquid fueled combustors". *Combustion and Flame,* ***205***, pp. 295–304.

[22] Carpenter, D., Nates, S., Dryer, F. L., and Won, S. H., 2021. "Evaluating ignition propensity of high cycloparaffinic content alternative jet fuel by a chemical functional group approach". *Combustion and Flame,* ***223***, pp. 243–253.